THE SUBMILLIMETER PROPERTIES OF THE 1 MS *CHANDRA* DEEP FIELD NORTH X-RAY SAMPLE

A. J. Barger,[1,2,3] L. L. Cowie,[1] A. T. Steffen,[2] A. E. Hornschemeier,[4] W. N. Brandt,[4] G. P. Garmire[4]
Submitted to the Astrophysical Journal Letters

ABSTRACT

We present submillimeter observations for 136 of the 370 X-ray sources detected in the 1 Ms exposure of the *Chandra* Deep Field North. Ten of the X-ray sources are significantly detected in the submillimeter. The average X-ray source in the sample has a significant 850 μm flux of 1.69 ± 0.27 mJy. This value shows little dependence on the $2 - 8$ keV flux from 5×10^{-16} erg cm^{-2} s^{-1} to 10^{-14} erg cm^{-2} s^{-1}. The ensemble of X-ray sources contribute about 10% of the extragalactic background light at 850 μm. The submillimeter excess is found to be strongest in the optically faint X-ray sources that are also seen at 20 cm, which is consistent with these X-ray sources being obscured and at high redshift ($z > 1$).

Subject headings: cosmology: observations — galaxies: evolution — galaxies: formation — galaxies: active

1. INTRODUCTION

Most of the energy density of the extragalactic X-ray background (XRB) resides in the hard X-ray band above 2 keV. Early $100 - 300$ ks *Chandra* observations, in combination with *ASCA* observations at the bright flux levels, resolved $> 60\%$ of the $2-10$ keV XRB into discrete sources (Mushotzky et al. 2001; Giacconi et al. 2001; Garmire et al. 2001a; Tozzi et al. 2001). Now two unprecedented 1 Ms *Chandra* exposures (Brandt et al. 2001; Rosati et al. 2001) have essentially completely resolved the remainder of the XRB at these hard energies.

Many of the hard X-ray sources in the ultradeep *Chandra* data appear to be highly absorbed systems with large hard to soft X-ray flux ratios. In these sources the rest-frame soft X-ray through near-infrared radiation is reprocessed by dust and gas surrounding the central active galactic nucleus (AGN), and the reradiated energy appears in the far-infrared (FIR). At high redshifts ($z > 1$) this FIR radiation is redshifted to the submillimeter and can be directly measured with the SCUBA camera (Holland et al. 1999) on the 15 m James Clerk Maxwell Telescope.

Early searches for submillimeter counterparts to *Chandra* X-ray sources yielded mixed results because of the small sample sizes: Fabian et al. (2000; A2390 and A1835) and Hornschemeier et al. (2000, 2001; Hubble Deep Field North and its vicinity) found no submillimeter counterparts to their hard X-ray sources, while Bautz et al. (2000; A370) found submillimeter counterparts to both of theirs. Barger et al. (2001a) used submillimeter data that covered the entire 57 arcmin^2 SSA13 *Chandra* X-ray field of Mushotzky et al. (2000) to look for overlaps between the hard X-ray and submillimeter populations. Although only one hard X-ray source was significantly detected in their submillimeter data, these authors found that the error-weighted sum of the submillimeter fluxes of all 20 hard X-ray sources in their sample was significant at 20 ± 6 mJy

and mostly arose from the $z > 1.5$ and spectroscopically unidentified sources.

In this paper we present submillimeter observations of the X-ray sources detected in the 1 Ms exposure of the *Chandra* Deep Field North (CDF-N). These data cover more than three times the area of the Barger et al. (2001a) submillimeter/X-ray data. Furthermore, the 1 Ms hard X-ray data go about a factor of 10 deeper than the 100 ks SSA13 data, providing a much larger sample with a wide dynamic range in X-ray flux. The 1 Ms X-ray source catalog presented in Brandt et al. (2001) contains 370 significantly detected point sources. Source positions are accurate to within $\approx 0.6 - 1.7''$, depending on the off-axis angle and the number of detected counts. For our analysis, we adopt from Table 3 of Brandt et al. (2001) the effective photon index (Γ) values, which are based on the ratio of the counts in the hard and soft bands, and the observed frame hard band flux values. The R magnitudes and redshifts are taken from the 1 Ms X-ray follow-up catalog of Barger et al. (2001b), which gives redshift identifications for 66 of the 136 X-ray sources with submillimeter observations.

2. SUBMILLIMETER OBSERVATIONS

SCUBA jiggle map observations at 850 μm were taken during observing runs in 2000 April and 2001 March and May. The maps were dithered to prevent any regions of the sky from repeatedly falling on bad bolometers. The chop throw was fixed at a position angle of 90 deg so that the negative beams would appear $45''$ on either side east-west of the positive beam. Regular "skydips" (Lightfoot et al. 1998) were obtained to measure the zenith atmospheric opacities, and the 225 GHz sky opacity was monitored at all times to check for sky stability. Pointing checks were performed every hour during the observations on the blazars 0923+392, 0954+685, 1144+402, 1216+487, 1219+285, 1308+326, or 1418+546. The data

[1]Institute for Astronomy, University of Hawaii, 2680 Woodlawn Drive, Honolulu, Hawaii 96822

[2]Department of Astronomy, University of Wisconsin-Madison, 475 North Charter Street, Madison, WI 53706

[3]Hubble Fellow and Chandra Fellow at Large

[4]Department of Astronomy & Astrophysics, 525 Davey Laboratory, The Pennsylvania State University, University Park, PA 16802

were calibrated using jiggle maps of the primary calibration source Mars or the secondary calibration sources CRL618, OH231.8+4.2, or 16293-2422. Submillimeter fluxes were measured using beam-weighted extraction routines that include both the positive and negative portions of the beam profile.

The data were reduced in a standard and consistent way using the dedicated SCUBA User Reduction Facility (SURF; Jenness & Lightfoot 1998). The new data were combined in the reduction process with the jiggle maps previously obtained by Barger, Cowie, & Richards (2000). Due to the variation in the density of bolometer samples across the maps, there is a rapid increase in the noise levels at the very edges, so the low exposure edges were clipped.

The SURF reduction routines arbitrarily normalize all the data maps in a reduction sequence to the central pixel of the first map; thus, the noise levels in a combined image are determined relative to the quality of the central pixel in the first map. In order to determine the absolute noise levels of our maps, we first eliminated the $\gtrsim 3\sigma$ real sources in each field by subtracting an appropriately normalized version of the beam profile. We then iteratively adjusted the noise normalization until the dispersion of the signal-to-noise ratio measured at random positions became ~ 1. The noise estimate includes both fainter sources and correlated noise.

3. SUBMILLIMETER FLUX MEASUREMENTS

The submillimeter fluxes of the X-ray sources were measured in an automated fashion. We first measured the submillimeter fluxes at the positions of the 20 cm $(> 3\sigma)$ sources from Richards (2000) that fell on our SCUBA maps. Any radio source that we detected above the 3σ level at 850 μm was included in a "detection list". We next measured all $> 5\sigma$ submillimeter sources that did not have a radio counterpart; we identified two and added them to the list. Finally, we added all the Chapman et al. (2001) submillimeter measurements (made in photometry mode) of radio sources that did not lie within our SCUBA jiggle maps.

After compiling the detection list, we compared the coordinates of the X-ray sources with the coordinates of the sources in the detection list. If an X-ray source was found to lie within $3''$ of a source in the detection list, we identified the list source as the counterpart to the X-ray source. All of the radio+submillimeter source counterparts had coordinates within $1.5''$ of the X-ray source positions. Once the cross-identifications were made, the sources in the detection list were removed from the SCUBA maps since the wide and complex beam patterns of the bright SCUBA sources can produce spurious detections at other positions. Submillimeter fluxes and uncertainties were then measured at all the unassigned X-ray positions using a recursive loop which removed X-ray sources that were detected in the submillimeter above the 3σ level in a descending order of significance prior to remeasuring the fluxes. This procedure again avoids multiple or spurious detections of a single bright submillimeter source.

Of the 370 *Chandra* X-ray sources in the CDF-N sample, 136 have 850 μm flux measurements with uncertainties less than 5 mJy and 109 have uncertainties less than 2.5 mJy. Five flux measurements were drawn from the Chapman et al. (2001) sample, including a significant 15.7 ± 2.4 mJy

detection. While we did not reproduce the submillimeter detection of one of the Chapman et al. sources which fell within our jiggle maps (VLA J123624+621743 was observed by Chapman et al. in poor weather conditions and found to be a marginal 3σ detection (see their Table 1); the source was also detected at the 3.7σ level in the scanmap of Borys et al. 2001), the very high significance of the 15.7 mJy source suggests that it is real. Complete exclusion of the Chapman et al. data has no significant effect on our subsequent analysis.

In total, we significantly $(> 3\sigma)$ detect in the submillimeter 10 of the 136 X-ray sources. The average submillimeter flux per X-ray source is 1.30 mJy, and the error-weighted average is 1.69 ± 0.16 mJy. The final submillimeter measurements are presented in the CDF-N 1 Ms X-ray follow-up catalog of Barger et al. (2001b) and are plotted versus hard X-ray flux (squares) in Figure 1. We include in the figure the SSA13 hard X-ray sources (circles) from Barger et al. (2001a) to better sample the bright, hard X-ray flux end.
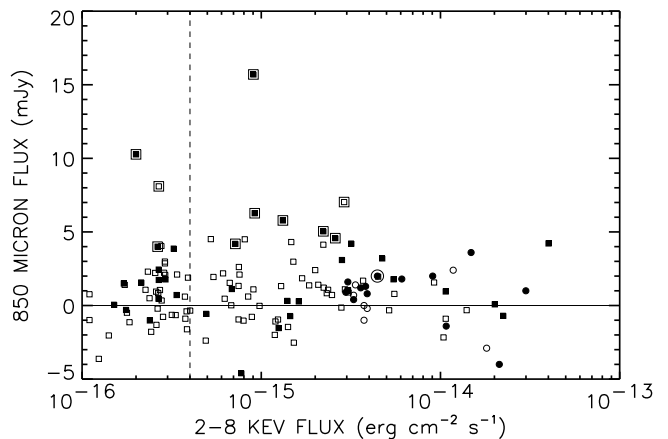

FIG. 1.— Submillimeter versus hard X-ray $(2-8$ keV) fluxes for the X-ray sources in the CDF-N (squares) and SSA13 (circles) fields with submillimeter measurements. Sources with $> 20\mu$Jy radio fluxes are denoted by filled symbols, and sources with $> 3\sigma$ submillimeter fluxes are denoted by a second large symbol. Thirty of the 46 sources to the left of the dashed vertical line at 4×10^{-16} erg cm^{-2} s^{-1} (including the two significant submillimeter sources that are also radio sources) are plotted at their hard X-ray flux limits. Two of these have hard X-ray flux limits less than 10^{-16} erg cm^{-2} s^{-1} and are shown at a nominal value of 1.1×10^{-16} erg cm^{-2} s^{-1}. Only one source to the right of the vertical line has only a hard X-ray flux limit $(1.25 \times 10^{-15}$ erg cm^{-2} s$^{-1})$.

In order to test the significance of our results, we repeated our submillimeter measurement procedure for a large number of simulations. In the simulations we offset the X-ray sample a random amount in the RA and Dec directions and then measured the submillimeter fluxes at these random positions. The average flux per source at these random positions was found to be accurately zero, but the dispersion from field to field was found to be 0.27 mJy rather than the nominal 0.16 mJy, suggesting the presence of some systematic error. We use this larger uncertainty subsequently. The 95 percent confidence level is 0.45 mJy, and the 98 percent confidence level is 0.6 mJy, leaving little doubt that there is a significant excess 850 μm flux associated with the X-ray sample. Similarly, the random samples have an average of 1.2 3σ sources per field

and 95 and 98 percent confidence levels of 4 and 5 sources, respectively, so most of the significantly detected submillimeter sources are real.

4. CONTRIBUTION TO THE SUBMILLIMETER EBL

The resolution of the FIR/submillimeter extragalactic background light (EBL) by the DIRBE and FIRAS experiments on *COBE* revealed that the FIR/submillimeter EBL has approximately the same integrated energy density as the optical EBL. Thus, the absorption and reradiation of light by dust in the history of galaxy formation and evolution is extremely important; however, in order to reconstruct the star formation and accretion histories of the Universe, we need to be able to differentiate between the FIR/submillimeter contributions made by starbursts and those made by AGN.

About $20 - 30$ percent of the 850 μm EBL has been resolved into discrete sources by blank field SCUBA surveys (e.g., Barger, Cowie, & Sanders 1999). Blain et al. (1999) estimated from a SCUBA survey of massive cluster lenses which amplify distant submillimeter sources that more than 80 percent of the 850 μm EBL is now resolved. The ultraluminous SCUBA sources are believed to be the high redshift analogs of the local ultraluminous infrared galaxies (ULIGs; Sanders & Mirabel 1996), but there is an ongoing debate even as to whether the local ULIGs are dominantly powered by star formation or by AGN activity. Modelling suggests that $\gtrsim 10 - 20$ percent of the FIR/submillimeter EBL may be contributed by galaxies containing bright AGN (Almaini, Lawrence, & Boyle 1999; Gunn & Shanks 2001). It is difficult to spectroscopically look for AGN signatures in the SCUBA sources — though in a few cases such signatures have been detected (e.g., Ivison et al. 1998; Barger et al. 1999) — due to the extremely faint nature of the vast majority of the optical counterparts. However, since most of the flux density from the *Chandra* X-ray sample is expected to arise from AGN activity, we may use the present data to place an upper limit on the AGN contribution to the 850 μm EBL. (A submillimeter source detected in X-rays is not necessarily solely powered by accretion onto the AGN, as there may also be dust obscured starburst activity in the galaxy which contributes to the submillimeter flux.)

Barger et al. (2001a) multiplied the hard XRB measurement from Vecchi et al. (1999) by the ratio of the total 850 μm flux to the total hard X-ray flux of the SSA13 hard X-ray sample to estimate the hard X-ray contribution to the 850 μm EBL. They determined the contribution to be about 10 percent. However, their approach assumed that a fixed submillimeter to X-ray flux ratio applies to all of the X-ray sources. We can quantitatively see that this is not a good assumption from Table 1, where we list the average X-ray flux and the average submillimeter flux and uncertainty for the CDF-N+SSA13 X-ray sources in each of four hard X-ray flux bins. Since the average submillimeter flux is consistent with being constant as a function of X-ray flux, the ratio of the submillimeter to X-ray flux rises with decreasing X-ray flux.

A better approach may be to translate the measured average 850 μm flux per X-ray source to an X-ray source contribution to the 850 μm EBL. The SCUBA jiggle maps cover an area of 194 arcmin^2. Excluding the Chapman et

al. (2001) sources, which lie outside this area, there are 131 X-ray selected sources with an average flux per source of 1.27 ± 0.27 mJy, where the uncertainty is again based on the random samples described in § 3. This translates to an 850 μm EBL of $3.1 \pm 0.66 \times 10^3$ mJy deg^{-2}, which is 10 ± 2 percent of the total 850 μm EBL, if we adopt the 3.1×10^4 mJy deg^{-2} value of Puget et al. (1996), or 7 ± 2 percent of the total, if we adopt the 4.4×10^4 mJy deg^{-2} value of Fixsen et al. (1998). Since our results indicate that the integrated 850 μm EBL is proportional to the total number of X-ray sources, the overall contribution to the EBL may increase with additional weaker X-ray sources. However, the rapid convergence of the X-ray number counts below 10^{-15} erg cm^{-2} s^{-1} (Garmire et al. 2001b) suggests that this correction would not be large.

5. SOURCE PROPERTIES

If the submillimeter flux represents the reprocessing of the radiated energy in the more obscured AGN, then we may expect to see a dependence of the submillimeter excess on X-ray hardness. However, an opposing tendency is introduced by redshift: 850 μm source detections are primarily expected to be at $z > 1$ because of the strong negative K-corrections at this wavelength that nearly compensate for cosmological dimming, while high redshift X-ray sources will appear softer in the observed frame than in the rest frame.
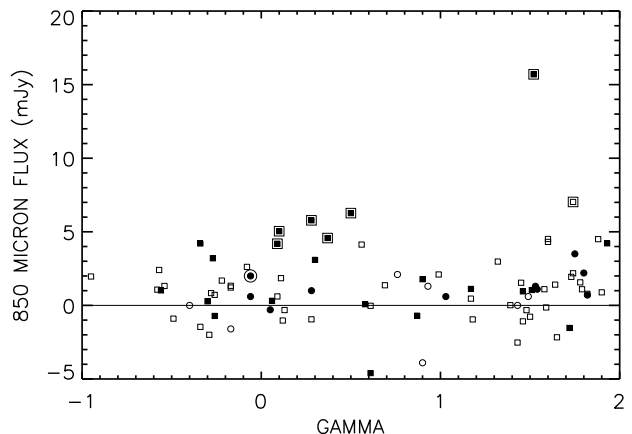

FIG. 2.— Submillimeter flux versus Γ for the X-ray sources in the CDF-N (squares) and SSA13 (circles) fields with hard X-ray fluxes above 5.0×10^{-16} erg cm^{-2} s^{-1}. Sources with $> 3\sigma$ radio fluxes are denoted by filled symbols, and sources with $> 3\sigma$ submillimeter fluxes are denoted by a second large symbol.

In Fig. 2 we plot 850 μm flux versus effective photon index for the nearly complete CDF-N hard X-ray sample (squares) above 5.0×10^{-16} erg cm^{-2} s^{-1} $(2 - 8$ keV), where the photon indices are well defined. We include on the figure the SSA13 hard X-ray sources (circles) from Barger et al. (2001a) to better sample the bright X-ray flux end. Of the eight significantly detected submillimeter sources which are present in this more restricted sample, six (including the SSA13 source) are clustered at low Γ values, which suggests they are obscured systems, while the remaining two (including a non-radio CDF-N source) have quite high Γ values, which suggests they are unobscured systems or obscured systems at high redshift. It should be kept in mind that we expect there to be one

or two spurious detections in the sample, so these objects could be false positives.

A more robust result can be obtained by considering the average properties of the sources. Dividing the CDF-N+SSA13 combined sample into hard sources with $\Gamma < 1$ and soft sources with $\Gamma > 1$, we find that the hard sources have an average submillimeter flux of 1.77 ± 0.21 mJy, which is substantially larger than the value of 0.89 ± 0.24 mJy in the soft sample. This suggests that most of the submillimeter flux is indeed coming from the obscured sources, although even the soft sources have a significant submillimeter excess.

In Fig. 3 we plot redshift versus submillimeter flux for the unrestricted CDF-N (squares) and SSA13 (circles) samples. Sources with spectroscopic redshifts are separated from sources without by two dotted lines at $z = 0$ and at $z = 3.5$. Below the $z = 0$ line, we plot the spectroscopically unidentified sources with magnitudes $R < 24.1$, which corresponds to the $I < 23.5$ definition of Barger et al. (2001a) for optically bright galaxies. These sources, although bright enough for spectroscopic identification, have not yet been observed; they will likely populate the same region of the plot as the low redshift sources. Above the $z = 3.5$ line, we plot the spectroscopically unidentified sources with magnitudes $R \geq 24.1$. These sources are generally too optically faint for spectroscopic identification. All but two of the significantly detected submillimeter sources fall into this region of the plot, which is consistent with the conclusion of previous SCUBA surveys that most submillimeter sources are optically faint. The two significantly detected submillimeter sources which are not optically faint have been observed spectroscopically: the spectrum for the $z = 1.013$ source, which is also a radio source, shows strong Balmer absorption features and [Ne III] in emission, so it appears to be a reliable identification, whereas the spectrum for the $z = 0.555$ source, which is not also a radio source, looks relatively normal, and thus its identification with the submillimeter source could be spurious.

Again it is instructive to consider the average submillimeter properties of the X-ray sources, this time according to redshift bin. The average submillimeter flux is significant in both the $z = 0$ to 1 (0.80 ± 0.21 mJy) and the $z = 1$ to 3.5 (1.09 ± 0.35 mJy) spectroscopic redshift bins. Moreover, the average submillimeter flux of the unidentified optically faint X-ray sources is highly significant (1.68 ± 0.19 mJy). The average submillimeter flux of the unidentified optically bright X-ray sources is not significant (0.72 ± 0.56 mJy) but is consistent with these sources populating the same region of the plot as the sources with spectroscopic redshifts.

Figure 3 shows how the unidentified optically faint X-ray sources tend to separate according to 850 μm flux into sources with radio counterparts and sources without. In fact, all but one of the significant SCUBA sources without a spectroscopic identification have radio counterparts. This result is again consistent with previous analyses of SCUBA data which found that targeted SCUBA surveys of optically faint radio sources are a far more efficient means of identifying SCUBA sources than random blank field surveys (Barger et al. 2000; Chapman et al. 2001).

Quantitatively, the average submillimeter flux of the optically faint X-ray sources with radio counterparts is 2.86 ± 0.28 mJy, which is significant at above the 10σ level. In contrast, the average submillimeter flux of the optically faint X-ray sources without radio counterparts is not significant (0.74 ± 0.25 mJy).

Figure 3 illustrates one additional property we can learn about the X-ray sources with significant submillimeter detections: their millimetric redshifts (Carilli & Yun 2000; Barger et al. 2000). We have overlaid on the data three curves which show the submillimeter flux dependence of a redshifted 20 μJy, 40 μJy, or 100 μJy radio source whose spectral energy distribution is assumed to be like that of the prototypical ULIG Arp 220. From these curves we can see that the unidentified optically faint sources that are significantly detected in the submillimeter are likely to fall in the redshift range between $z = 1$ and 3.
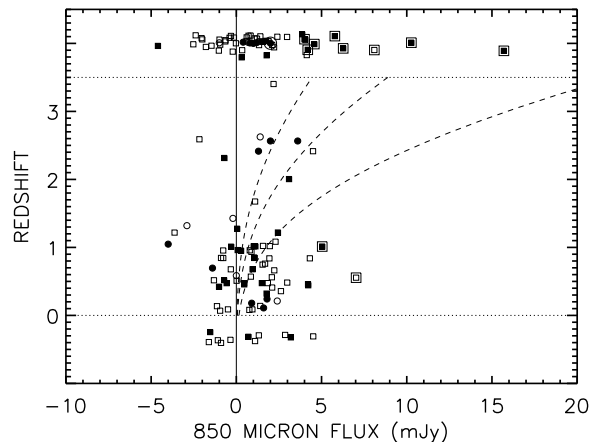

FIG. 3.— Redshift versus submillimeter flux for the X-ray sources in the CDF-N (squares) and SSA13 (circles) fields. Sources with $> 3\sigma$ radio fluxes are denoted by filled symbols, and sources with $> 3\sigma$ submillimeter fluxes are denoted by a second large symbol. Sources without spectroscopic identifications are plotted at either the bottom of the figure (the optical counterparts have magnitudes $R < 24.1$) or at the top of the figure (the optical counterparts have magnitudes $R \geq 24.1$), separated from the spectroscopically identified data by the dotted lines. Overlaid on the data are three dashed curves which show the expected tracks of a redshifted 20 μJy (leftmost curve), 40 μJy, and 100 μJy radio source, assuming a spectral energy distribution like that of the ultraluminous infrared galaxy Arp 220.

TABLE 1

AVERAGE FLUXES FOR THE CDF-N+SSA13 SAMPLE IN FOUR X-RAY FLUX BINS

$f(2-8 \text{ keV})$ Bin (10^{-16} ergs cm^{-2} s^{-1})	Average $f(2-8 \text{ keV})$ (10^{-16} ergs cm^{-2} s^{-1})	Average $f(850 \ \mu\text{m})$ (mJy)
$5-10$	7.5	1.7 ± 0.32
$10-30$	20	1.8 ± 0.29
$30-100$	44	1.3 ± 0.27
$100-500$	180	0.25 ± 0.42

REFERENCES

Almaini, O., Lawrence, A., & Boyle, B. J. 1999, MNRAS, 305, L59
Barger, A. J., Cowie, L. L., & Sanders, D. B. 1999, ApJ, 518, L5
Barger, A. J., Cowie, L.L., Smail, I., Ivison, R. J., Blain, A. W., & Kneib, J.-P. 1999, AJ, 117, 2656
Barger, A. J., Cowie, L. L., & Richards, E. A. 2000, AJ, 119, 2092
Barger, A. J., Cowie, L. L., Mushotzky, R. F., & Richards, E. A. 2001a, AJ, 121, 662
Barger, A. J., et al. 2001b, in preparation
Bautz, M. W., Malm, M. R., Baganoff, F. K., Ricker, G. R., Canizares, C. R., Brandt, W. N., Hornschemeier, A. E., & Garmire, G. P. 2000, ApJ, 543, L119
Blain, A. W., Smail, I., Ivison, R. J., & Kneib, J.-P. 1999, MNRAS, 302, 632
Borys, C., Chapman, S. C., Halpern, M., & Scott, D. 2001, MNRAS, submitted
Brandt, W. N., et al. 2001, AJ, submitted
Carilli, C. L. & Yun, M. S. 2000, ApJ, 539, 1024
Chapman, S. C., Richards, E.A., Lewis, G. F., Wilson, G., & Barger, A. J. 2001, ApJ, 551, L9
Fabian, A. C., et al. 2000, MNRAS, 315, L8
Fixsen, D. J., Dwek, E., Mather, J. C., Bennett, C. L., & Shafer, R. A. 1998, ApJ, 508, 123

Garmire, G. P., et al. 2001a, ApJ, submitted
Garmire, G. P., et al. 2001b, in preparation
Giacconi, R., et al. 2001, ApJ, 551, 624
Gunn, K. F. & Shanks, T. 2001, MNRAS, submitted
Holland, W. S., et al. 1999, MNRAS, 303, 659
Hornschemeier, A. E., et al. 2000, ApJ, 541, 49
Hornschemeier, A. E., et al. 2001, ApJ, 554, 742
Ivison, R. J., Smail, I., Le Borgne, J.-F., Blain, A. W., Kneib, J.-P., Bézecourt, J., Kerr, T.H., & Davies, J.K. 1998, MNRAS, 298, 583
Jenness, T. & Lightfoot, J. F. 1998, Starlink User Note 216.3
Lightfoot, J. F., Jenness, T., Holland, W. S., & Gear, W. K. 1998, SCUBA System Note 1.2
Mushotzky, R. F., Cowie, L. L., Barger, A. J., & Arnaud, K. A. 2000, Nature, 404, 459
Puget, J.-L., Abergel, A., Bernard, J.-P., Boulanger, F., Burton, W. B., Desert, F.-X., & Hartmann, D. 1996, A&A, 308, L5
Richards, E. A. 2000, ApJ, 533, 611
Rosati, P., et al. 2001, in preparation
Sanders, D.B. & Mirabel, I.F. 1996, ARA&A, 34, 749
Tozzi, P., et al. 2001, ApJ, in press, (astro-ph/0103014)
Vecchi, A., Molendi, S., Guainazzi, M., Fiore, F., & Parmar, A. N. 1999, A&A, 349, L73